Rock Petrophysical Properties and Modeling

Sources for Core Analysis Data

As with many smaller Mississippian fields, core was not available from within the field. To provide models for predicting permeability, oil-water relative permeability, capillary pressure properties, and connate water saturations, regional petrophysical trends for the Mississippian and trends obtained from analysis of eight cores from nearby fields were used.

Porosities for the Wellington West field average 16±4%. Porosities are interparticle, intraparticle and moldic. Properties of the moldic porosity rocks are largely controlled by original depositional fabric with permeablity increasing from mudstones to grainstones.

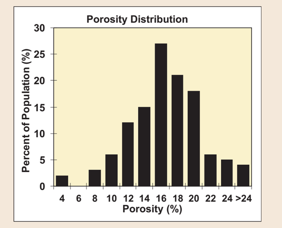

Lithofacies, Permeability, Porosity

Lithofacies and early diagenesis are major controls on permeability (k) and porosity ( ) despite complex diagenetic overprinting by sub-Pennsylvanian subaerial exposure and burial processes.

- k and decrease significantly and continuously with decreasing grain/mold size from packstone to mudstone (a trend exhibited by many other carbonates) and from echinoderm-rich to spicule-rich facies

The permeability-porosity trend for all lithofacies are approximately bounded within two orders of magnitude by trendlines defined by:

$\log k_{in\ situ} = 0.25 \quad _{in\ situ} - 2.5$

$\log k_{in\ situ} = 0.25 \quad _{in\ situ} - 4.5$

- Between these bounding trends each lithofacies exhibits a generally unique range of k and which together define a continuous trend with k decreasing with decreasing grain/mold size for any given porosity. Each individual lithofacies exhibits a unique sub-parallel trend to the general trend. Statistically the general trend is dominated by the large number of spicule-rich samples and is strongly influenced by mudstone and cemented echinoderm grainstone properties:

$\log k_{in\ situ}\ (md) = 0.24 \quad _{in\ situ}(\%) - 3.78$

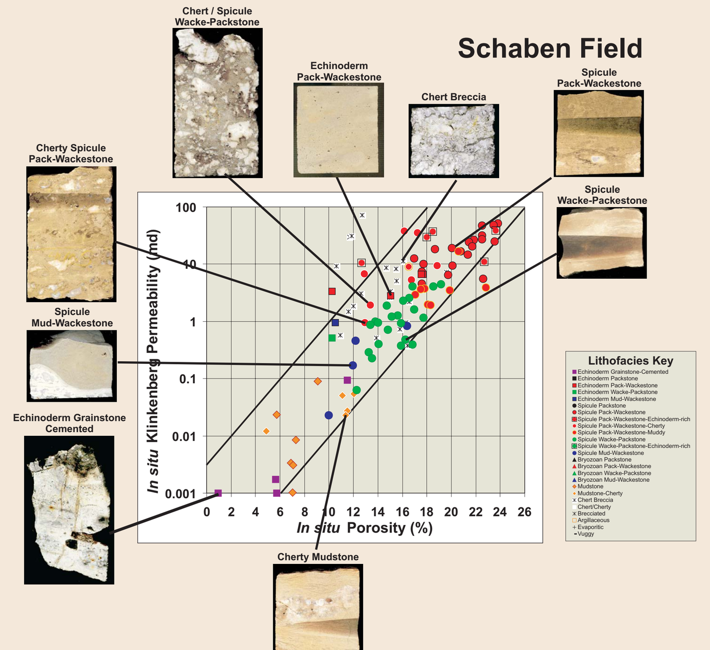

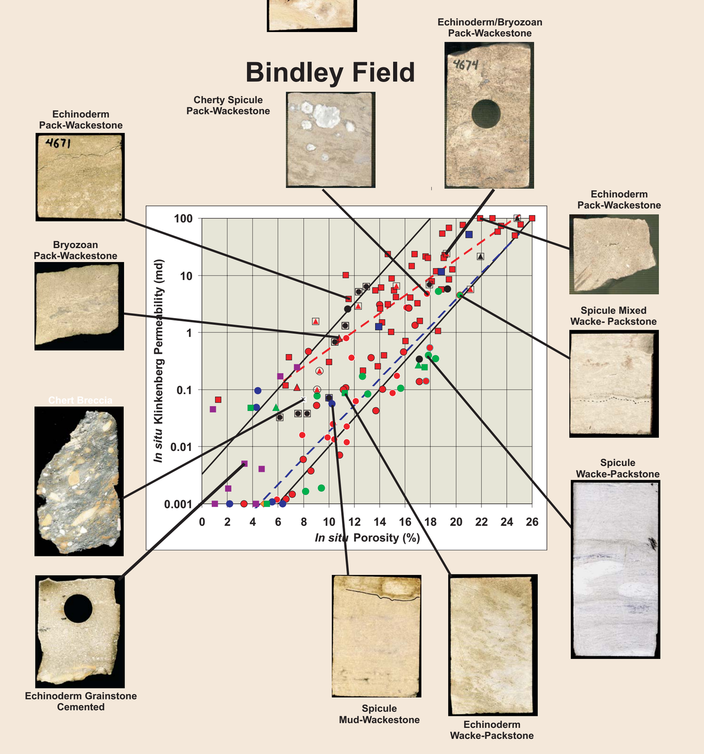

Wellington West Equations

Wireline log response was able to to identify dolomite, limestone, and chert facies but could not distinguish lithofacies (mudstone-grainstone). Permeability-porosity (k-) trends for cores from eight wells in nearby fields were consistent with regional Mississippian trends. It was assumed that these trends were most representative of the Wellington West field. Permeability for the carbonates was predicted from porosity using:

Dolomite: $ki = 0.746\ e^{0.189}$

Limestone: $ki = 0.00198\ e^{0.569}$

Local cherts exhibit a k- trend (light blue line) that is subparallel to the regional chert trend (blue line). Because of limited local sampling the regional trend was considered more robust and was utilized for modeling.

Chert regional: $ki = 0.0309\ e^{0.166}$

Chert: $ki = 0.000894\ e^{0.273}$

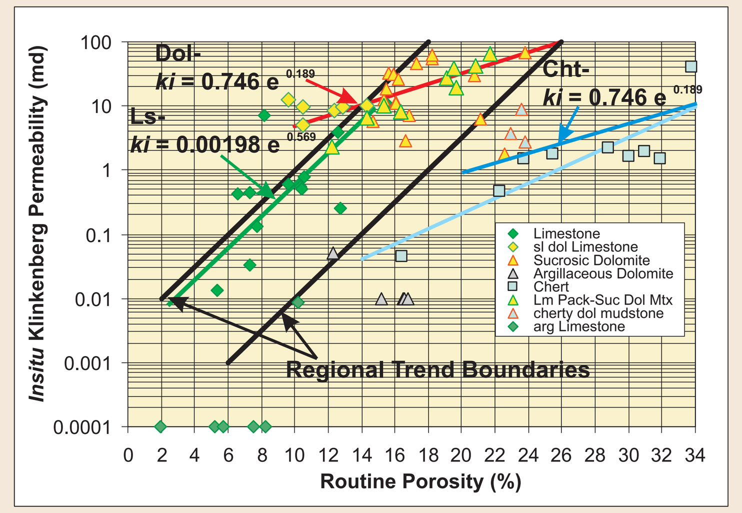

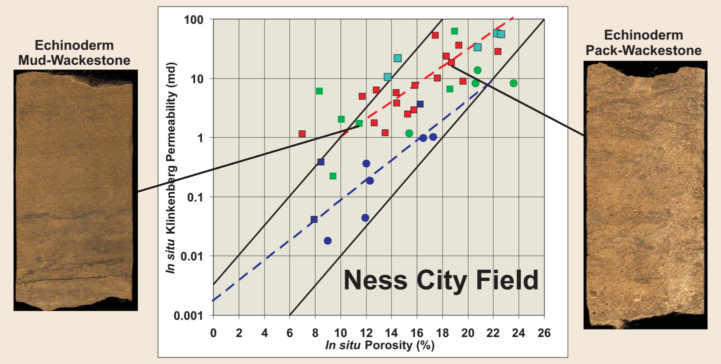

Permeability and Pore Throats

Though permeability is shown correlated with porosity, variables that control permeability in Mississippian rocks include pore throat size and distribution, grain size distribution, moldic pore size and packing, and moldic pore connectivity. Porosity is only one of the variables controlling permeability and bivariate correlation therefore relies on the correlation between porosity and the other controlling variables. A crossplot of permeability and principal pore throat diameter (PPTD) illustrates the control PPTD exerts on permeability.

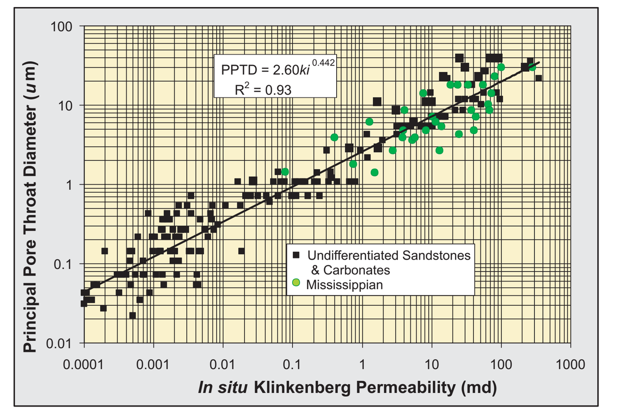

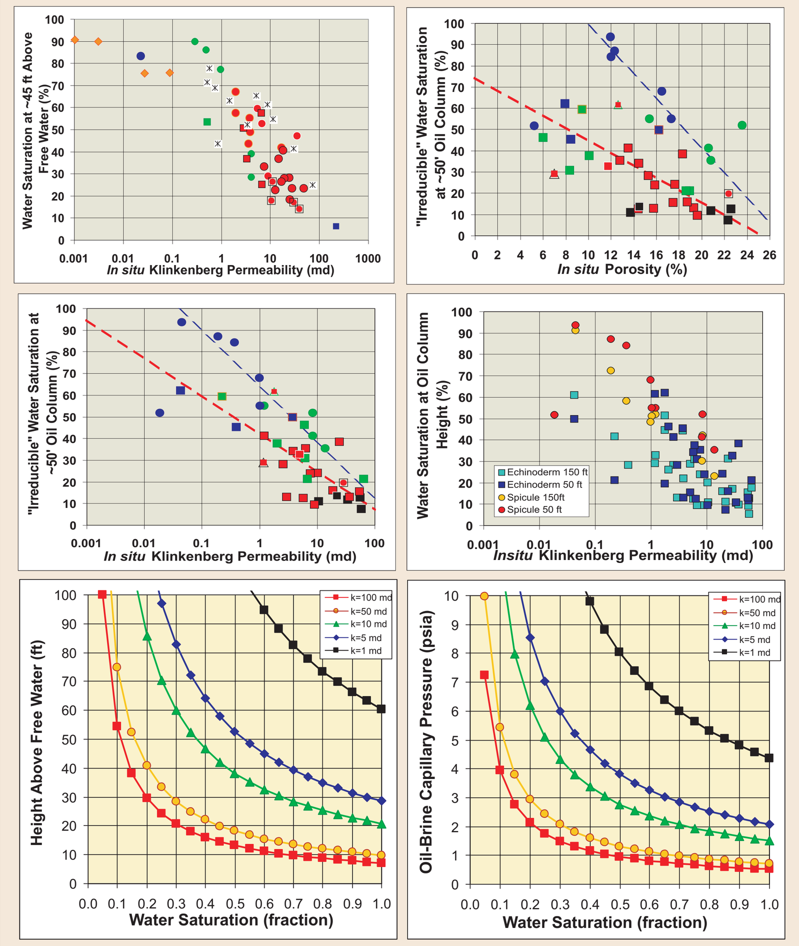

Capillary Pressure

Fluid saturations in the Wellington West field were determined using electrical wireline logs and capillary pressure relations. Capillary pressure curves show a relationship of increasing threshold entry pressure with decreasing permeability that is consistent with decreasing pore throat size with decreasing permeability (Figure). Capillary pressure properties of Mississippian carbonates differ between lithofacies. Structural closure in many Mississippian Kansas fields is less than 60 feet limiting oil column heights and necessitating understanding of the exact capillary pressure relationships.

Air-brine capillary pressure measurements indicate that water saturations at 45-50 ft (Sw45,Sw50) above free water increase with decreasing porosity and permeability (Figures). Because of the close correlation between lithofacies and k- , Sw also increase with decreasing grain/mold size from packstone to mudstone. Sw45 in Schaben can be predicted within ± 14% (saturation %) using: Sw45(%) = -20*log *kinsitu* + 61. Within the echinoderm-rich facies in Ness Field, S_{w50} is correlated with and **k**: Sw50(%) = -3.21 *insitu* + 87.6l (SE=±19%) and Sw50(%) = -17.5 $\log_{10}$ *kinsitu* + 42.1 for Echinoderm-rich facies (SE=±8.7).

For cores near Wellington West the following relations predicts Sw60:

Sw60(%) = -28.8 $\log_{10}$ *kinsitu* + 62.6.

Generalized Capillary Pressure Curves

To provide capillary pressure curves for the reservoir simulation it was necessary to develop generalized curves that represented the specific permeabilities that might be assigned to a gridcell. Equations to construct generalized capillary pressure curves were constructed based on the relationships evident from the entry pressures and curve shapes in the air-mercury capillary pressure curves, and from the saturations evident in the air-brine capillary pressure analysis. The relationships between increasing entry pressure, "irreducible" wetting phase saturation, and the capillary curve curvature (reflecting increasing pore throat size heterogeneity) with decreasing permeability were utilized to develop equations that would predict the capillary pressure curve using permeability as the independent variable.

Entry pressure, or the first pressure at which wetting phase desaturation begins and similar to R35, exhibits a strong correlation with permeability and can be predicted using:

$$Pcow_{entry} = 4.374\ ki^{-0.4625}$$

Where $Pcow_{entry}$ is the oil-water entry pressure and **ki** is the *in situ* permeability. Using the above term and a function to model capillary pressure curve shape synthetic capillary pressure curves could be created for any permeability.

Modeling Relative Permeability

Since relative permeability end point saturations change with permeability (e.g., "irreducible" water saturation changes with permeability), the relative permeability curves also change with absolute permeability. Relative permeability curves for any given permeability were modeled using Corey-type equations where ***Swi*** was obtained from ***Pc-k*** relations and the average absolute permeability values assigned. Exponent ***m*** and ***n*** values were initially obtained from measured data and were modified during simulation to reproduce lease production data.

$$kro = {}_1(1-S_{wD})^m$$
$$krw = {}_2 S_{wD}^{\ n}$$
$$S_{wD} = (S_w - S_{wi})/(1 - S_{wi} - S_{orw})$$

For moldic-porosity Mississippian rocks residual oil saturation to waterflood also changes with permeability and/or Swi following the general trend: Sorw=(1-(Swi+0.5)). Initial pseudo-***Swi*** values were assigned to each layer using ***Pc-k*** relations discussed.

Figures show how kro and krw change with permeability. The lower figures on right

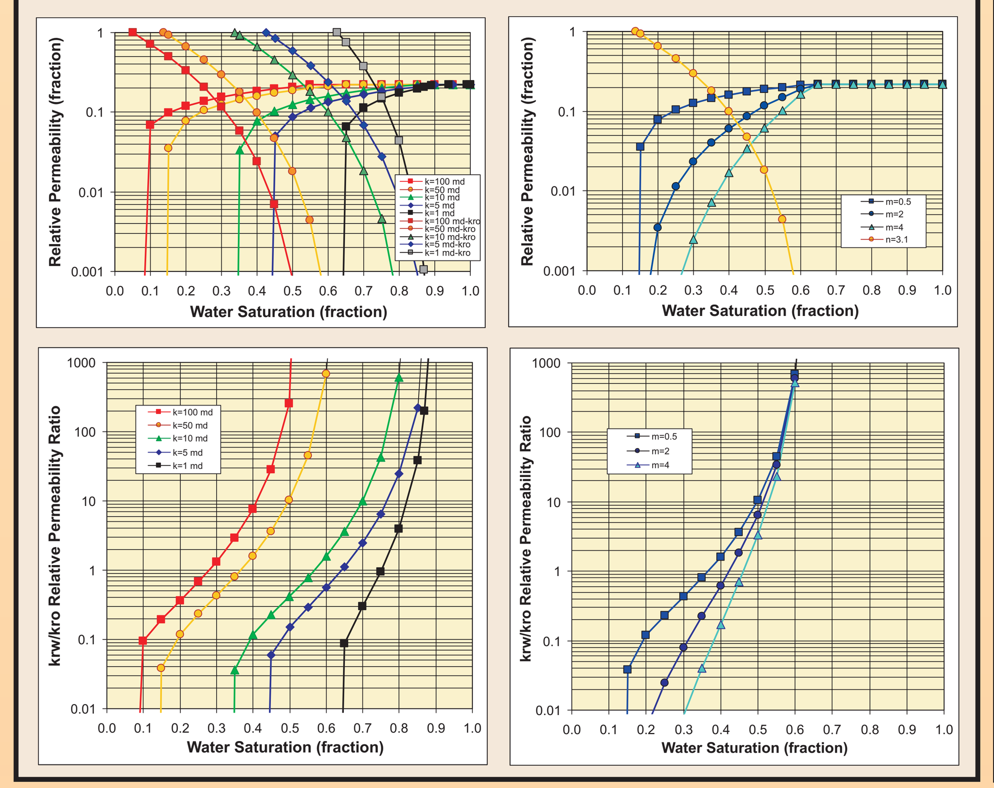

Calculator for Wellington West

K(md)=	100				
Krwmax=	100	Kromax=	1	Pce=	0.520
Krw -m=	0.5	Swi=	0.05	Pcs=	-0.879
Kro - n=	3.1	Sorw=	0.450	PcSwiH(ft)=	60.0
water grad	0.438	W sp grav=	1.0111	input value	
oil grad	0.365	Oil sp grav=	0.8439	calc value	

SW	KRW	KROW	PCOW	Height above free water (ft)	SwD
0.0500	0.0000	1.0000	7.236	99.94	0.00000
0.1000	31.4960	0.7233	3.934	54.34	0.09920
0.1500	44.6318	0.5023	2.755	38.05	0.19920
0.2000	54.6992	0.3322	2.139	29.55	0.29920
0.2500	63.1823	0.2061	1.758	24.29	0.39920
0.3000	70.6541	0.1172	1.498	20.69	0.49920
0.3500	77.4080	0.0588	1.308	18.07	0.59920
0.4000	83.6182	0.0241	1.163	16.07	0.69920
0.4500	89.3980	0.0069	1.049	14.49	0.79920
0.5000	94.8262	0.0008	0.956	13.21	0.89920
0.5500	99.9600	0.0000	0.879	12.14	0.99920
0.6000	100.0000	0.0000	0.814	11.25	1.00000
0.6500	100.0000	0.0000	0.759	10.49	1.00000
0.7000	100.0000	0.0000	0.711	9.82	1.00000
0.7500	100.0000	0.0000	0.669	9.25	1.00000
0.8000	100.0000	0.0000	0.633	8.74	1.00000
0.8500	100.0000	0.0000	0.600	8.28	1.00000
0.9000	100.0000	0.0000	0.570	7.88	1.00000
0.9500	100.0000	0.0000	0.544	7.51	1.00000
1.0000	100.0000	0.0000	0.520	7.18	1.00000
1.0000	100.0000	0.0000	0.520	7.18	1.00000

To facilitate simulator modification and history matching an Excel worksheet was constructed that contained all relevant equations linked to porosity and/or permeability. With this worksheet, if the simulator required an adjustment of the permeability, the corresponding capillary pressure and relative permeability properties could be calculated and input. This kept all petrophysical properties "coupled." This worksheet also provided easy changes to relative permeability and immediate feed-back of the effect of a change on flow at a given saturation.

Wellington West dolomites exhibit a general increase in pore body size with increasing k as shown by Nuclear Magnetic Resonance T2 times.

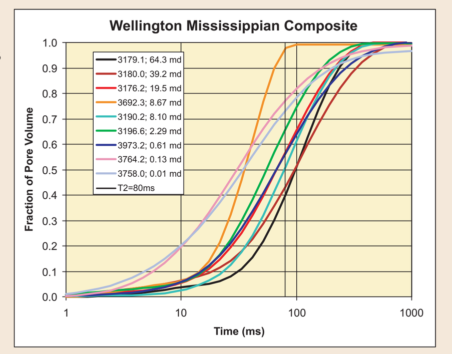

Archie Cementation Exponent

Traditional wireline log calculation of saturations use the Archie equation and cementation (m) and saturation exponent (n) values of 2. Formation resistivity factors (Ro/Rw) measured at Rw=0.045 ohm-m (Figure) indicate that the Archie cementation exponent (assuming an Archie intercept of 1.0) averages m=1.97+0.09 for all facies. Echinoderm-rich facies can exhibit cementation exponents between 2.0 and 2.1. Vuggy cherts can exhibit cementation exponents between 2.1 and 2.2.

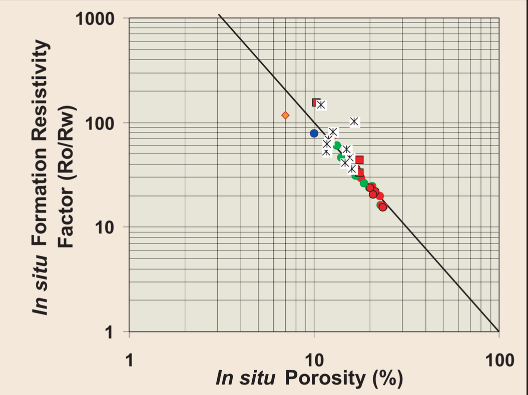

Production data

Field production recorded by lease
Wharton Lease - 3 wells
Becker Lease - 2 wells
Waugh Lease - 6 wells

Barrel test (Oil & Water) data available from 1989 to date - 1 test per year

Field developed between 1977 to 1985
Majority of wells drilled in 1983

Initial oil production history missing in each well

How to reconstruct oil production history?

Advanced Decline Curve Analyses

Match available production (rate/time) data with a model.

Production data normally includes both transient and depletion declines

- **Transient - decline caused by fluid expansion with continually increasing drainage area**
- **Depletion - decline after drainage radius reaches outer boundaries**

Decline curves analyse production data from depletion period only.

Used to estimate missing production data or to predict future production provided production practices remain unchanged.

This method estimates reserve volumes that are in pressure communication - ultimately recoverable by the wells.

Type curves, theoretical solutions to flow equations, are often used for decline analyses.

Fetkovich decline type curves were used here.

Model assumptions

- **Well producing under constant BHP**
- **Well is centered in a circular drainage area**
- **No-flow occurs at drainage boundaries**

Reconstruct Oil Production History Advanced Decline Curve Analyses

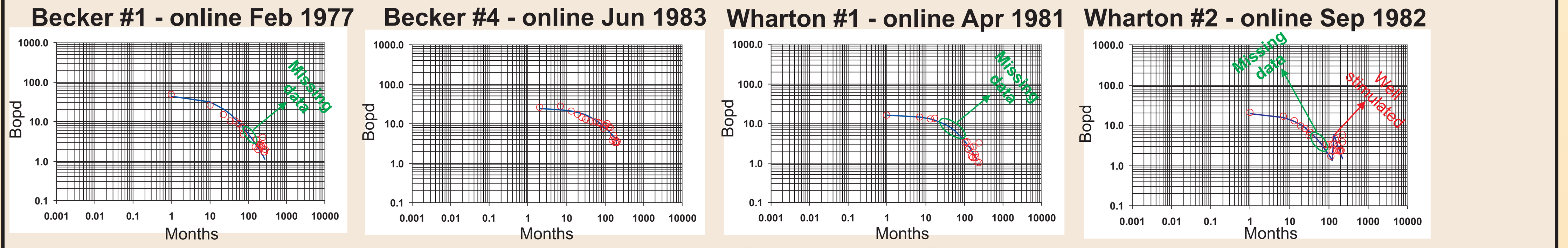

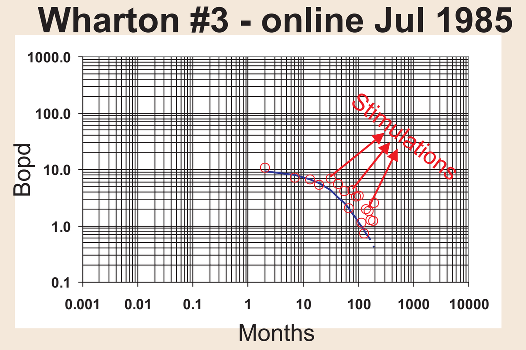

Missing oil production between 1983 to 1988 estimated for Becker #1 - completed oil history.
Production history for Becker #4 completed between 1983 to 1988 by subtraction Becker #1 production from Becker Lease.
Reconstructed Becker #4 history also falls on a decline curve.

Oil production histories reconstructed for Wharton #1 & #2.
Oil production for Wharton #3 during 1985-89 estimated by subtracting production from Wharton #1 & #2 from lease production.
Reconstructed production history for Wharton #3 falls on a decline curve and indicates intermittent stimulations.

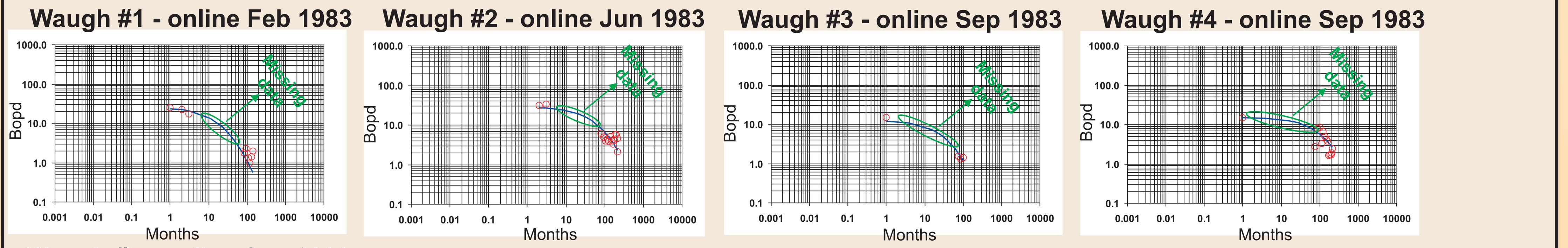

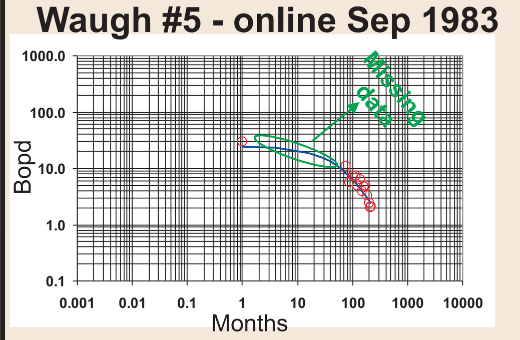

Inferences from Decline Curve Analyses

Oil production histories were completed using initial production (IP) rates and barrel test data recorded since 1989.
Reconstructed oil production data from wells in a lease when added together closely approximated recorded lease production.
Available production data, for most of the productive life of each well, could be modeled by a decline curve. This means that bottom hole producing pressures (Pwfs) at the wells remained mostly unchanged.
Recorded production data at some of the wells indicated that wells underwent intermittent stimulations.
A very short transient decline is visible when the recorded production data is plotted on Fetkovich's Type Curve. This is indicative of low effective permeabilities existing in the reservoir.

Water Production data

Available water production data consisted of IP (initial production) records from Scout cards and annual barrel test results from 1989. The IP records show that measureable amounts of water were recorded in only 4 wells - Waugh #5, #6, #7, and Wharton #3. Of these 4 wells, water rates greater than 2 bbls/day were recorded in only 2 wells. It appears that initial water production from remaining wells were not significant enough to merit measurement and record.

Based on this limited water production data, it is not unreasonable to assume that initial water saturation in the reservoir was at "*critical water saturation*", S_{wcrit}, where the relative permeability to water, K_{rw},is effectively zero (or close to zero as perhaps is the case in this field).

Summary of IP rates from Scout Cards

Well	KB	Perforation from, ft	Perforation to, ft	Perf from Subsea, ft	Perf to Subsea, ft	IP bopd	IP bwpd	Acidization
Wharton 1	1237	3644	3658	-2407	-2421	15		Yes
Wharton 2	1244	3646	3660	-2402	-2416	25	No Water	Yes
Wharton 3	1246	3654	3664	-2408	-2418	25	10	Yes
Becker 1	1246	3790	3800	-2544	-2554	50		Yes
Becker 4	1248	3652	3670	-2404	-2422	25	Water	Yes
Waugh 1	1258	3654	3670	-2396	-2412	25		Yes
Waugh 2	1252	3652	3656	-2400	-2404	25	Water	Yes
Waugh 3	1248	3644	3662	-2396	-2414	15	Water	Yes
Waugh 4	1259	3672	3686	-2413	-2427	15		Yes
Waugh 5	1245	3660	3670	-2415	-2425	30	2	Yes
Waugh 6	1257	3655	3656	-2398	-2399	25	25	Yes
Waugh 7	1256	3680	3685	-2424	-2429	25	1	Yes